Computational Geosciences **8:** 49–73, 2004.

Modelling two-phase incompressible flow in porous media using mixed hybrid and discontinuous finite elements

D. Nayagum [a], G. Schäfer [a,b,*] and R. Mosé [c]

[a] *Institut de Mécanique des Fluides et des Solides, UMR 7507 ULP-CNRS, 2 rue Boussingault, 67000 Strasbourg, France*
E-mail: schafer@imfs.u-strasbg.fr
[b] *Institut Franco-Allemand de Recherche sur l'Environnement (IFARE), 23 rue du Loess, B.P 20, 67037 Strasbourg Cedex, France*
[c] *Ecole Nationale du Génie de l'Eau et de l'Environnement, 1 quai Koch, 67000 Strasbourg, France*

Received 6 September 2002; accepted 26 January 2004

In this paper, we present a numerical model for simulating two-phase (oil–water and air–water) incompressible and immiscible flow in porous media. The mathematical model which is based on a fractional flow formulation is formed of two nonlinear partial differential equations: a mean pressure equation and a water saturation equation. These two equations can be solved in a sequential manner. Two numerical methods are used to discretize the equations of the two-phase flow model: mixed hybrid finite elements are used to treat the pressure equation, h-based Richards' equation and the diffusion term in the saturation equation, the advection term in the saturation equation is treated with the discontinuous finite elements. We propose a better way to calculate the nonlinear coefficients contained in our equations on each element of the discretized domain. In heterogeneous porous media, the saturation becomes discontinuous at the interface between two porous media. We show in this paper how to use the capillary pressure–saturation relationship in order to handle the saturation jump in the mixed hybrid finite element method. The two-phase flow simulator is verified against analytical solutions for some flow problems treated by other authors.

Keywords: fractional flow formulation, mixed hybrid and discontinuous finite elements, porous media, two-phase flow

1. Introduction

Two-phase flow is encountered in the fields of hydrology and petroleum engineering. In order to predict the infiltration of water and calculate the quantity of water present in the soil matrix often needed for agricultural purposes, the air–water two-phase model system is considered. The two-phase water–oil system arising in the petroleum industry has been extensively studied since the works of Buckley and Leverett [5]. There are two approaches to modelling two-phase flow in porous media. The first one is based on the

* Corresponding author.

individual balance equations of the fluids while the second one implies rearrangement and manipulation of those individual equations and introduction of new functions like the fractional flow function. Following the first approach, the water–oil two-phase system can be modelled by two pressure equations obtained after substitution of Darcy's velocity of each fluid phase into the individual mass balance equations. This pressure-pressure system of equations can be transformed into a pressure–saturation form by using the relationship between the capillary pressure which is the difference between the phase pressures and the saturation. The pressure of the second phase can then be removed by expressing it in terms of the saturation and pressure of the other phase. This latter approach is useful when phase disappearance occurs and the saturation of that phase becomes zero. The system of partial differential equations describing two-phase flow is highly nonlinear due to the nature of the permeability and capillary pressure functions needed to close the system.

Alternative forms of the governing equations have been investigated in order to apply better computational algorithms. This led to the fractional flow approach which originates from the petroleum industry. In this approach, we consider the total fluid flow then describe the individual phases as a fraction of the total flow. Through the fractional flow formulation, the immiscible displacement of oil and water can be expressed in terms of two coupled equations, a mean pressure equation or global pressure equation usually and a saturation equation [3,7,11,12]. The fractional flow approach will be adopted in this work because the pressure and the saturation equations can be treated in a sequential manner. The coupling between these two equations is looser than with the pressure–pressure or the pressure–saturation formulations where the system of equations have to be solved simultaneously. The pressure equation is an elliptic partial differential equation whereas the saturation equation is of advection–diffusion type.

The pressure equation can be solved by a variety of numerical techniques, however due to large variations of the permeability field, the pressure field varies extremely on short distances. The velocity field may contain large errors if it is calculated through differentiation of the pressure field. The mixed hybrid finite element method by providing a simultaneous approximation of the pressure and the velocity field is very attractive. Furthermore, the velocity field which is needed in a second step to solve the advective part of the saturation equation has a continuous normal component from one element to the other. Mixed methods have been shown to be superior to solve the pressure equation compared to conventional methods [1,12].

For the reasons exposed previously, the pressure equation of the two-phase system will be solved by the mixed hybrid method. The saturation which is of advection–diffusion type will be solved by an operator splitting technique. Advection and diffusion will be treated separately, the advective term is solved using the discontinuous finite element method [2,7,23] with an explicit in time scheme and the diffusive term is solved via a mixed hybrid method. For the special case of flow of air and water for which we consider the air phase as infinitely mobile, Richards' equation [22] is used to model the two-phase system. The nonlinear parabolic differential equation modelling this simplified two-phase water–air system is solved by the mixed hybrid finite element with a time

implicit scheme. The nonlinear system of equations is linearized using a standard Picard technique.

In this study, we examine the calculation of a highly nonlinear diffusive associated coefficient contained in our equations. We show that by evaluating this coefficient by its arithmetic mean value on the element edges, far better results can be achieved for some two-phase flow problems. Numerical treatment of the saturation equation by the mixed hybrid finite element is complicated by the discontinuity of the saturation at the interface between two porous media. At this point of changing porous material, the capillary pressure remains continuous if we use the capillary pressure–saturation function of Van Genuchten [26] and it can become discontinuous with the Brooks and Corey function. If we use the Brooks and Corey function, we have to distinguish two cases: if the capillary pressure in the coarser medium at the point of discontinuity is greater than the entry pressure corresponding to that material then the capillary pressure should be considered as continuous, if we have the other case then the capillary pressure should be considered as discontinuous.

The numerical simulator is verified through comparison with analytical solutions for classical water–oil flow problems studied by [5] and [15]. The two-phase incompressible flow simulator is tested for an unsaturated flow problem studied by several authors [6,13,14,20]. For model verification in heterogeneous porous media, we consider the horizontal distribution of oil and water in a horizontal column filled with two porous media. We use the capillary pressure–saturation relationship of Brooks and Corey [4] to model this counter current displacement. The usual continuity of the trace of the unknown variable has to be modified by writing the continuity or discontinuity of the capillary pressure on the element edge found at the interface between two porous media. Finally, our numerical solution is compared to the analytical one for this problem proposed by [25].

2. The mathematical model

The mathematical model is based on the mass balance equation for each phase of the two-phase system:

$$\frac{\partial(\phi\rho_\alpha S_\alpha)}{\partial t} + \nabla\cdot(\rho_\alpha \boldsymbol{v}_\alpha) + q_\alpha = 0, \tag{1}$$

where $\phi(-)$ is the porosity, ρ_α is the fluid density (ML^{-3}), S_α is the degree of saturation ($\mathrm{L}^3\mathrm{L}^{-3}$), q_α is the source or sink term ($\mathrm{ML}^{-3}\mathrm{T}^{-1}$) and the fluid phase velocity $\boldsymbol{v}_\alpha$ (LT^{-1}) is given by Darcy's generalized law:

$$\boldsymbol{v}_\alpha = -\frac{k_{\mathrm{r}\alpha}}{\mu_\alpha}\boldsymbol{K}\cdot(\nabla p_\alpha - \rho_\alpha \boldsymbol{g}), \tag{2}$$

where p_α is the pressure of phase α ($\mathrm{ML^{-1}T^{-2}}$), $k_{r\alpha}$ is the relative permeability to fluid phase α; μ_α is the dynamic viscosity of fluid α ($\mathrm{ML^{-1}T^{-1}}$), $\boldsymbol{K}$ is the permeability tensor ($\mathrm{L^2}$) and the gravity vector $\mathbf{g}$ [$\mathrm{LT^{-2}}$] is defined as

$$\boldsymbol{g} = \begin{bmatrix} 0 \\ 0 \\ -g \end{bmatrix}. \tag{3}$$

Through manipulation of the mass balance equations and Darcy's law, and using the fact that the saturations sum to one, the incompressible two-phase system can be modelled by a mean pressure (p_m) equation [11,17]:

$$\nabla \cdot \boldsymbol{v}_\mathrm{t} = Q_\mathrm{t}, \tag{4}$$

where the total velocity $\boldsymbol{v}_\mathrm{t}$ is given by

$$\boldsymbol{v}_\mathrm{t} = -\lambda_\mathrm{t}\boldsymbol{K} \cdot \nabla p_\mathrm{m} - \frac{1}{2}(\lambda_\mathrm{n} - \lambda_\mathrm{w})\boldsymbol{K} \cdot \nabla p_\mathrm{c} + (\lambda_\mathrm{n}\rho_\mathrm{n} + \lambda_\mathrm{w}\rho_\mathrm{w})\boldsymbol{K}\boldsymbol{g}, \tag{5}$$

and a water saturation (S_w) equation

$$\phi\frac{\partial S_\mathrm{w}}{\partial t} = \nabla \cdot (\boldsymbol{h}_\mathrm{w} \cdot \nabla S_\mathrm{w}) - \nabla \cdot (f_\mathrm{w}\boldsymbol{v}_\mathrm{t}) - \nabla \cdot \boldsymbol{G}_\mathrm{w} + Q_\mathrm{w}. \tag{6}$$

In the above equations, the following definitions are used:

$$p_\mathrm{m} = \frac{p_\mathrm{w} + p_\mathrm{n}}{2}, \tag{6a}$$

$$\lambda_\mathrm{t} = \frac{k_\mathrm{rw}}{\mu_\mathrm{w}} + \frac{k_\mathrm{rn}}{\mu_\mathrm{n}}, \tag{6b}$$

$$Q_\mathrm{t} = -\left(\frac{q_\mathrm{w}}{\rho_\mathrm{w}} + \frac{q_\mathrm{n}}{\rho_\mathrm{n}}\right), \tag{6c}$$

$$\boldsymbol{h}_\mathrm{w} = -\lambda_\mathrm{n} f_\mathrm{w}\boldsymbol{K}\frac{\mathrm{d}p_\mathrm{c}}{\mathrm{d}S_\mathrm{w}} \equiv -\sigma(S_\mathrm{w})\boldsymbol{K}, \tag{6d}$$

$$f_\mathrm{w} = \frac{\lambda_\mathrm{w} + \lambda_\mathrm{n}}{\lambda_\mathrm{t}}, \tag{6e}$$

$$\boldsymbol{G}_\mathrm{w} = f_\mathrm{w}\lambda_\mathrm{t}(\rho_\mathrm{w} - \rho_\mathrm{n})\boldsymbol{K}\boldsymbol{g}, \tag{6f}$$

where p_m is the mean pressure of oil and water [$\mathrm{ML^{-1}T^{-2}}$], λ_t is the total mobility of oil and water ($\mathrm{M^{-1}LT}$), Q_t is the total volumetric flux ($\mathrm{L^3T^{-1}L^{-3}}$), $\boldsymbol{h}_\mathrm{w}$ is the diffusion coefficient ($\mathrm{L^2T^{-1}}$), f_w is the fractional flow function for water (–) and G_w is the gravity function ($\mathrm{LT^{-1}}$). The capillary pressure ($\mathrm{ML^{-1}T^{-2}}$) and the source/sink term ($\mathrm{L^3T^{-1}L^{-3}}$) are denoted by p_c and Q_w, respectively.

Constitutive relationships relating the water saturation to the capillary pressure and the relative permeability $k_{r\alpha}$ need to be introduced in order to close the system of equa-

tions (equations (5), (6)) of the two-phase flow model. The saturation–capillary pressure relationship of Brooks and Corey [4] is given by:

$$S_e \equiv \frac{S_w - S_{wr}}{1 - S_{nr} - S_{wr}} = \left(\frac{p_d}{p_c}\right)^{\lambda} \quad \text{with } p_c \geqslant p_d, \tag{7}$$

and the relative permeabilities of oil and water are related to the water saturation by

$$k_{rw} = S_e^{(2+3\lambda)/\lambda} \tag{8}$$

and

$$k_{rn} = (1 - S_e)^2\left(1 - S_e^{(2+\lambda)/\lambda}\right). \tag{9}$$

In the above expressions, S_e is the effective water saturation, S_{nr} is the residual saturation for oil (L^3L^{-3}), S_{wr} is the residual water saturation (L^3L^{-3}), λ is the pore size index (–), and p_d is the entry pressure ($ML^{-1}T^{-2}$) which corresponds to the minimum pressure needed by the oil phase to displace the water phase.

The air–water two-phase system is classically simplified and modelled by Richards' equation which is obtained by writing the mass balance equation (1) for water and replacing the water phase velocity by its Darcy's expression:

$$\frac{\partial\theta}{\partial t} - \nabla \cdot \left[\overline{\boldsymbol{K}}(h)\nabla(h + z)\right] = 0, \tag{10}$$

where the moisture content θ (L^3L^{-3}) is given by $\theta = \phi S_w$, the unsaturated hydraulic conductivity $\overline{\boldsymbol{K}}(h)$ (LT^{-1}) is given by $\overline{\boldsymbol{K}}(h) = \lambda_w \boldsymbol{K}\rho_w g = k_{rw}K_s$, where $\boldsymbol{K}_s$ is the saturated hydraulic conductivity, the water pressure expressed in height of column of water is given by $h = p_w/\rho_w g$ (L) and z is the vertical coordinate (L).

We employ the h-based formulation of Richards' equation:

$$C(h)\frac{\partial h}{\partial t} - \nabla \cdot \left[\overline{\boldsymbol{K}}(h)\nabla(h + z)\right] = 0, \tag{11}$$

in which $C(h) = \partial\theta/\partial h$ is the specific moisture content (L^{-1}).

The effective water saturation S_e can also be expressed in terms of the water content:

$$S_e = \frac{\theta - \theta_r}{\theta_s - \theta_r}, \tag{12}$$

where θ_r (L^3L^{-3}) and θ_s (L^3L^{-3}) are the residual and saturated water content, respectively.

Relationships of Mualem [16] and Van Genuchten [26] are used to express the dependence of the water pressure and the relative permeability on the effective water saturation by

$$S_e = \begin{cases} \dfrac{1}{[1 + (\alpha|h|)^n]^{1-1/n}} & \text{if } h \leqslant 0, \\ 1 & \text{if } h \geqslant 0 \end{cases} \tag{13}$$

and

$$k_{\mathrm{rw}} = S_{\mathrm{e}}^{1/2}\left[1 - \left(1 - S_{\mathrm{e}}^{1/m}\right)^{m}\right]^{2} \quad \text{if } h \leqslant 0, \tag{14}$$

with

$$m = 1 - \frac{1}{n}. \tag{15}$$

Empirical constants α (L^{-1}) and n (–) determine the shape of the functions used.

3. Numerical treatment

In this section, we will consider the numerical resolution of the system of equations modelling two-phase flow in porous media. Two discretization techniques are used to discretize our equations: the mixed hybrid finite element method (MHFE) and the discontinuous finite element method (DFE). These two numerical techniques have been chosen for the reasons exposed in the introductory part of this paper. The diffusive and the advective term in the saturation equation are treated separately via a time operator splitting technique [10]. The MHFE technique is applied to solve the elliptic mean pressure equation, the parabolic diffusive part contained in the saturation equation and Richards' equation. The time scheme used is implicit. Advection in the saturation equation is solved by the DFE with an explicit time scheme. In order to prevent undershooting or overshooting of the calculated saturations with respect to adjacent cells, slope limiters are implemented. Our system of highly nonlinear equations is linearized using a standard Picard technique.

3.1. Brief description of numerical methods used

In this work, we have developed a 2-D numerical tool in order to simulate more realistic practical problems.

3.1.1. DFE applied to the resolution of advection

The advective part of the saturation equation

$$\phi \frac{\partial S_{\mathrm{w}}}{\partial t} = -\nabla \cdot (f_{\mathrm{w}} \boldsymbol{v}_{\mathrm{t}}), \tag{16}$$

is solved using the DFE method with an explicit in time second order accurate scheme. A slope limiting procedure is associated with the DFE to eliminate numerical instabilities while introducing only a small numerical diffusion. We refer to the papers of [7] and [23] for a detailed presentation of the method.

The 2-D domain is discretized with quadrangular elements, the water saturation S_{w} is approximated using a space M of discontinuous bilinear functions

$$M = \left\{ f\big|_{E} \in (m_{E_1}, m_{E_2}, \ldots, m_{E_4}) \right\}. \tag{17}$$

Inside an element E, the water saturation is given by

$$S_E(x, y) = \sum_{i=1}^{4} m_{E_i} S_E^i, \tag{18}$$

where S_E^i is the value of the water saturation at node i of element E and m_{E_i} are basis bilinear functions of Galerkin type taking on the reference element a value of 1 at node i and 0 elsewhere.

We now introduce the following approximations:

- $S_{E_i}^{\text{in}}$ is the linear variation of the water saturation on edge E_i considered inside element E,
- $S_{E_i}^{\text{out}}$ is the linear variation of the water saturation on edge E_i considered outside of element E (inside the neighbour element E').

The hyperbolic equation (16) is solved in three steps.

Step 1. Calculation of $S_E^{n+1/2}$ using the interior values in E at time step $t^{n+1/2} = t^n + \Delta t_n/2$.

$$\int_E \frac{S_E^{n+1/2} - S_E^n}{1/2\Delta t_n} m = \int_E f_{\text{w}}\big(S_E^n\big)(\boldsymbol{U} \cdot \nabla m) - \sum_1^4 \int_{E_i} f_{\text{w}}\big(S_{E_i}^n\big) m \boldsymbol{U} \cdot \boldsymbol{n}_{E_i}$$

$$\text{with} \quad \boldsymbol{U} = \sum_{i=1}^{4} \overline{Q}_{E_i} \boldsymbol{w}_i. \tag{19}$$

$\boldsymbol{U} = \boldsymbol{v}_{\text{t}}/\phi$ is the real total velocity of the two phases (LT^{-1}) and $\overline{Q}_{E_i} = Q_{E_i}/\phi$ is the total real flux (L^2T^{-1}) through edge E_i. In equation (19), m denotes one of the basis functions m_{E_i}, $\boldsymbol{w}_i$ (L^{-1}) are the lowest order Raviart–Thomas space (RT^0) vector basis functions [21] (see equations (27) and (28)) and $S_{E_i}^n$ is a linear variation of the water saturation on edge E_i using interior values of the saturations at the corresponding nodes.

Using successively the basis functions m_{E_i} on element E, we obtain a system of 4 equations with four unknowns per element. The values of $S_{E_i}^{i,n+1/2}$ for each node i of element E are calculated by solving the local system of equations.

Step 2. Calculation of $S_E^{n+1^*}$ by solving the Riemann problem at time step t^{n+1}.

$$\int_E \frac{S_E^{n+1^*} - S_E^n}{\Delta t_n} m = \int_E f_{\text{w}}\big(S_E^{n+1/2}\big)(\boldsymbol{U} \cdot \nabla m) - \sum_1^4 \int_{E_i} f_{\text{w}}\big(\widetilde{S}_{E_i}^{n+1/2}\big) m \boldsymbol{U} \cdot \boldsymbol{n}_{E_i}. \tag{20}$$

In this step, the advective numerical flux is evaluated using upstream values of S_{w} at the interface between two elements. The linear variation of the saturation $\widetilde{S}_{E_i}^{n+1/2}$ on edge E_i denotes here either $S_{E_i}^{\text{in}}$ or $S_{E_i}^{\text{out}}$ which are the linear variations of the saturation on edge E_i inside and outside element E, respectively. The choice between $S_{E_i}^{\text{in}}$ and $S_{E_i}^{\text{out}}$ depends on the sign of the flux:

- if $\overline{Q}_{E_i} \geqslant 0$, $S_{E_i} = S_{E_i}^{\text{in}}$,
- if $\overline{Q}_{E_i} < 0$, $S_{E_i} = S_{E_i}^{\text{out}}$.

Step 3. Calculation of S_E^{n+1} by stabilisation of the solution using slope limiters at time step t^{n+1}. The scheme is stabilised using multidimensional slope limiters. The following notations are introduced:

- $\overline{S}_E = \left(\sum_{i=1}^{4} S_E^i\right)/4$, is the mean value of S_{w} in the element,
- $\min(i)$ is the minimum of $\overline{S}_E^{n+1^*}$ of all elements containing node i,
- $\max(i)$ is the maximum of $\overline{S}_E^{n+1^*}$ of all elements containing node i,
- $\min(E)$ is the minimum of $\overline{S}_E^{n+1^*}$ of all elements sharing a node with element E,
- $\max(E)$ is the maximum of $\overline{S}_E^{n+1^*}$ of all elements sharing a node with element E.

The multidimensional slope limiting operator L associates to each S^{n+1^*} the function $L(S^{n+1^*}) = S^{n+1}$ which satisfies the following condition:

$$\overline{S}_E^{n+1} = \overline{S}_E^{n+1^*}, \tag{21}$$

for mass conservation.

In order to reduce variations, we apply the following constraints:

$$\min(i) \leqslant S_E^{i,n+1} \leqslant \max(i), \tag{22}$$

$$S_E^{i,n+1} = \overline{S}_E^{n+1^*} \quad \text{if } \overline{S}_E^{n+1^*} \geqslant \max(E) \quad \text{or} \quad \overline{S}_E^{n+1^*} \leqslant \min(E). \tag{23}$$

If both conditions in equation (23) are not satisfied, then $S_E^{i,n+1}$ is not defined uniquely. To get a unique solution, we impose $S_E^{i,n+1}$ to be the closest to $S_E^{i,n+1^*}$ by minimising the objective function J defined by

$$J\left(S_E^{i,n+1}\right) = \sum_{i=1}^{4} \left\| S_E^{i,n+1} - S_E^{i,n+1^*} \right\|^2. \tag{24}$$

The saddle point method [9] is used to minimise the objective function while respecting the constraints on $S_E^{i,n+1}$. Our scheme being explicit with respect to time, we need to respect a criterion on the Courant–Friedrich–Levy number (CFL < 1) to get a stable solution.

3.1.2. MHFE applied to the resolution of diffusion

In this section, we will expose only the treatment of the diffusive part of the saturation equation together with the gravity and the source/sink terms. The mean pressure equation and Richards' equation are solved by the MHFE technique in a similar way [17].

The part of the saturation equation to be solved is given by

$$\phi \frac{\partial S_{\mathrm{w}}}{\partial t} = \nabla \cdot (\boldsymbol{h}_{\mathrm{w}} \cdot \nabla S_{\mathrm{w}}) - \nabla \cdot \boldsymbol{G}_{\mathrm{w}} + Q_{\mathrm{w}}. \tag{25}$$

We introduce a diffusive water flux $\boldsymbol{q}_{\mathrm{d}}$ (LT^{-1}) defined by

$$\boldsymbol{q}_{\mathrm{d}} = -\sigma(S_{\mathrm{w}})\boldsymbol{K} \cdot \nabla S_{\mathrm{w}}. \tag{26}$$

Our 2-D space domain Ω is discretized with quadrangular elements. To describe the mixed method we introduce the lowest order Raviart–Thomas space (RT^0) vector basis functions $\boldsymbol{w}_i$ (L^{-1}) [21] which have the following properties:

$$\int_{A_j} \boldsymbol{w}_i \cdot \boldsymbol{n}_{A_j} \,\mathrm{d}s = \delta_{ij}, \quad 1 \leqslant i, j \leqslant 4, \tag{27}$$

and

$$\int_E \nabla \cdot \boldsymbol{w}_i \,\mathrm{d}x = \sum_{i=1}^{4} \int_{A_j} \boldsymbol{w}_i \cdot \boldsymbol{n}_{A_j} = 1, \tag{28}$$

where $\boldsymbol{n}_{A_j}$ is the normal unit vector to edge A_j belonging to element E and δ_{ij} is the Kronecker symbol. The vector $\boldsymbol{w}_i$ has a flux equal to one through edge A_i and a zero flux through all other edges.

Let $\boldsymbol{q}_{\mathrm{d}E}$ be an approximation of the diffusive flux $\boldsymbol{q}_{\mathrm{d}}$ on element E, then $\boldsymbol{q}_{\mathrm{d}E}$ can be expressed in the Raviart–Thomas space by

$$\boldsymbol{q}_{\mathrm{d}E} = \sum_{j=1}^{4} Q_{E_j} \boldsymbol{w}_j, \tag{29}$$

Q_{E_j} being the flux over edge A_j.

We introduce now the following spatial approximations:

- S_E is an approximation of the mean water saturation S_{w} on element E,
- TS_{E_i} is an approximation of the mean water saturation on the edge A_i of the element E,
- σ_E is the mean value of $\sigma(S_{\mathrm{w}})$ on element E.

Using a variational formulation and the $\boldsymbol{w}_i$ as weighting functions, the diffusive flux can be written as

$$Q_{\mathrm{d},E_i} = S_E \alpha_{\mathrm{d},E_i} - \sum_{j=1}^{4} B^{-1}_{\mathrm{d},E_{ij}} TS_{E_j}, \tag{30}$$

where

$$\alpha_{\mathrm{d},E_i} = \sum_{j=1}^{4} B_{\mathrm{d},E_j} = \sum_{j=1}^{4} \left[\sigma_E^{-1} \int_E \left(\boldsymbol{K}^{-1} \boldsymbol{w}_j \right) \cdot \boldsymbol{w}_i \right] \tag{31}$$

with $\sigma_E > 0$.

The diffusive flux of water entering or leaving each element E at a discrete time t^{n+1} is given by

$$\int_E \nabla \cdot \boldsymbol{q}_{\mathrm{d},E}^{n+1} = \int_E \nabla \cdot \left(\sum_{i=1}^{4} Q_{\mathrm{d},E_i}^{n+1} \boldsymbol{w}_i \right) = \sum_{i=1}^{4} Q_{\mathrm{d},E_i}^{n+1} \int_E \nabla \cdot \boldsymbol{w}_i = \sum_{A_i \subset \partial E} Q_{\mathrm{d},E_i}^{n+1}. \tag{32}$$

Equation (25) is discretized on each element E with an implicit Euler time scheme:

$$\phi |E| \frac{S_E^{n+1} - S_E^n}{\Delta t} + \int_E \nabla \cdot \boldsymbol{q}_{\mathrm{d},E}^{n+1} + \int_E \nabla \cdot \boldsymbol{G}_{\mathrm{w}}^{n+1} = \int_E Q_{\mathrm{w}}^n. \tag{33}$$

By expressing the diffusive flux across each edge of an element, and using the expression of the gravity flux with the divergence theorem, equation (33) can be written as

$$\phi |E| \frac{S_E^{n+1} - S_E^n}{\Delta t} + \sum_{i=1}^{4} Q_{\mathrm{d},E_i}^{n+1} + \int_{\partial E} \boldsymbol{G}_{\mathrm{w}}^{n+1} \cdot \boldsymbol{n}_{\partial E} = \int_E Q_{\mathrm{w}}^n, \tag{34}$$

or

$$\phi |E| \frac{S_E^{n+1} - S_E^n}{\Delta t} + \alpha_{\mathrm{d},E} S_E^{n+1} - \sum_{j=1}^{4} \alpha_{\mathrm{d},E_j} T S_{E_j}^{n+1} + G_{\mathrm{w},E}^{n+1} = F_{\mathrm{w},E}^n, \tag{35}$$

with

$$\alpha_{\mathrm{d},E} = \sum_{i=1}^{4} \alpha_{\mathrm{d},E_i}, \tag{36}$$

$$F_{\mathrm{w},E}^n = \int_E Q_{\mathrm{w}}^n \tag{37}$$

and

$$G_{\mathrm{w},E}^{n+1} = \int_{\partial E} \boldsymbol{G}_{\mathrm{w}}^{n+1} \cdot \boldsymbol{n}_{\partial E} = \int_{\partial E} \widetilde{G}_{\mathrm{w}}^{n+1} (\boldsymbol{K} \cdot \nabla z) \cdot \boldsymbol{n}_{\partial E} = \sum_{i=1}^{4} T\widetilde{G}_{E_i}^{n+1} \int_{A_i} (\boldsymbol{K} \cdot \nabla z) \cdot \boldsymbol{n}_{A_i}. \tag{38}$$

In equation (38), $T\widetilde{G}_{E_i}^{n+1}$ is a mean value of $\widetilde{G}_{\mathrm{w}}^{n+1}$ on edge A_i, with

$$T\widetilde{G}_{E_i}^{n+1} = T\widetilde{G}_{E_i}^{n+1}\left(TS_{E_i}^{n+1}\right) = f_{\mathrm{w}}\left(TS_{E_i}^{n+1}\right) \lambda_{\mathrm{n}}\left(TS_{E_i}^{n+1}\right) (\rho_{\mathrm{n}} - \rho_{\mathrm{w}}) g. \tag{39}$$

By regrouping the mean water saturation on element E at time t^{n+1} and replacing the resulting expression in equation (30), the water flux on edge A_i is given by

$$Q_{\mathrm{d},E_i}^{n+1} = \frac{\phi |E|}{\Delta t} H_{\mathrm{d},E_i} S_E^n + H_{\mathrm{d},E_i} \left(F_{\mathrm{w},E}^n - G_{\mathrm{w},E}^{n+1} \right) + H_{\mathrm{d},E_i} \sum_{j=1}^{n_f} \alpha_{\mathrm{d},E_j} T S_{E_j}^{n+1} - \sum_{j=1}^{n_f} B_{\mathrm{d},E_{ij}}^{-1} T S_{E_j}^{n+1}, \tag{40}$$

with

$$H_{\mathrm{d},E_i} = \frac{\alpha_{\mathrm{d},E_i}}{\phi|E|/\Delta t + \alpha_{\mathrm{d},E}}. \tag{41}$$

To construct the mixed hybrid system we write the continuity of diffusive fluxes Q_{d,E_i}^{n+1} and water saturation traces $TS_{E_j}^{n+1}$ on non imposed edges. We remark here that the last condition on the continuity of saturations is true only in a homogeneous medium. In heterogeneous media, the extended pressure condition introduced by [25] should be used on edges found at the interface between the two porous media (see section 3.3).

The mixed hybrid approximation of equation (25) can be written finally as

$$\left(M_{ij}^{S,\mathrm{MH}} - N_{ij}^{S,\mathrm{MH}}\right)TS^{n+1} = F_i^{S,\mathrm{MH}} - R_i^{S,\mathrm{MH}}, \tag{42}$$

where the following definitions are used:

$$M_{ij}^{S,\mathrm{MH}} = \sum_{E\supset A_i,A_j} B_{\mathrm{d},E_{ij}}^{-1}, \tag{43}$$

$$N_{ij}^{S,\mathrm{MH}} = \sum_{E\supset A_i,A_j} H_{\mathrm{d},E_i}\alpha_{\mathrm{d},E_j}, \tag{44}$$

$$\begin{aligned} F_i^{S,\mathrm{MH}} = {} & \sum_{E\supset A_i} H_{\mathrm{d},E_i}\left(F_{\mathrm{w},E}^{n} - G_{\mathrm{w},E}^{n+1}\right) + \sum_{E\supset A_i} H_{\mathrm{d},E_i}\frac{|E|\phi_E}{\Delta t}S_E^n \\ & - \left[\sum_{E\supset A_i,A_j,\ A_j\subset\Gamma_D} B_{\mathrm{d},E_{ij}}^{-1} - \sum_{E\supset A_i,A_j,\ A_j\subset\Gamma_D} H_{\mathrm{d},E_i}\alpha_{\mathrm{d},E_j}\right]TS_{E_j}^{n+1}, \end{aligned} \tag{45}$$

$$R_i^{S,\mathrm{MH}} = \begin{cases} Q_{N,A_i}^{n+1}, & \text{for } A_i \subset \Gamma_N, \\ 0. \end{cases} \tag{46}$$

The unknowns of the system of equations of equation (42) are the water saturation traces. The associated matrix is symmetric and defined positive with dimension [NF × NF], NF being the number of edges with non-imposed saturation.

3.2. Approximation of nonlinear coefficients

In equation (26), the diffusion associated coefficient $\sigma(S_{\mathrm{w}})$ is a highly nonlinear function of the water saturation S_{w}. The water saturation $S_{\mathrm{w}}(X,t)$ being itself a space and time function implies that $\sigma(S_{\mathrm{w}})$ will also be a function of these two variables. Two spatial approximations are used to evaluate $\sigma(S_{\mathrm{w}})$ on each element, firstly using the saturation traces TS_{E_i} which we call approach A:

$$\sigma_E = \frac{1}{4}\sum_{i=1}^{4}\sigma(TS_{E_i}), \tag{47}$$

and secondly using the mean value of saturations on the elements S_E which we call approach B:

$$\sigma_E = \sigma(S_E). \tag{48}$$

Choosing between approach A or B can lead to very different results as is shown in section 4.

The two spatial approximations shown above have also been extended to the calculation of the specific moisture content $C(h)$ and the unsaturated hydraulic conductivity $\overline{\boldsymbol{K}}(h)$ in the resolution of the h-based Richards' equation with the mixed hybrid finite element method. With approach A, we use the mean water pressure on the element edges to evaluate the coefficients, while with approach B, the mean water pressure values on each element are used.

3.3. Treatment of the saturation discontinuity with the mixed finite element method

Let us consider a two phase flow problem in a heterogeneous porous media of two different permeabilities (figure 1). At the limit between these two porous media, two conditions must be applied [25]. Firstly, the flux must be continuous at the interface and secondly, the extended pressure condition should be applied. The last condition implies that there exists a relationship between the right-hand side saturation TS_{r} and the left-hand side one TS_{l} of the interface [8]. This means the relationship between these two saturations values depends on the function used for the capillary pressure–saturation relationship. The entry pressure P_{d} used in the Brooks and Corey model (BC) plays an important role in the description of two phase flow. This entry pressure corresponds to the minimum pressure that must be exerted by the non wetting phase to displace the wetting phase present initially in the porous media. If the entry pressure is positive, then the capillary pressure can be discontinuous at the limit between two porous media.

Let us suppose that medium 1 is made of a coarse sand with greater permeability than medium 2 which is composed of fine sand. Furthermore, we suppose that the entry

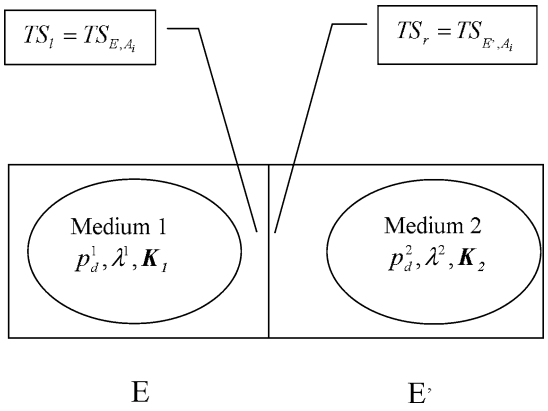

Figure 1. Saturation discontinuity at the interface between two porous media.

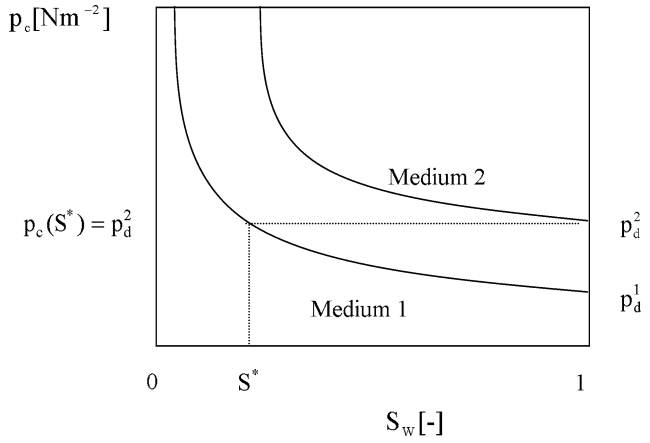

Figure 2. p_c–S_w relationship of the Brooks and Corey model for two different porous media.

pressure and the residual saturation for medium 2 are greater than those for medium 1. For simplicity we assume that the residual saturation for oil, $S_{nr} = 0$ for the two sands. We now study the horizontal displacement of water by the non-aqueous phase, the direction of the displacement being from the left to the right. By analyzing the capillary pressure–saturation curve from the Brooks and Corey model (figure 2), we can make the following remarks:

(1) If the water saturation in medium 1 is greater than S^*, then the saturation in medium 2 is equal to 1. The capillary pressure becomes discontinuous and is equal to p_d^2.

$$\text{If } TS_l > S^* \quad \text{then } TS_r = 1 \tag{49}$$

and

$$p_c(TS_l) \neq p_c(TS_r) = p_d^2. \tag{50}$$

(2) If the water saturation in medium 1 is lower than S^*, then the right-hand side saturation will be a function of the left-hand side one. The capillary pressure remains continuous.

$$\text{If } TS_l < S^* \quad \text{then } TS_r = f(TS_l) \tag{51}$$

and

$$p_c(TS_l) = p_c(TS_r). \tag{52}$$

We should remark here that with the Van Genuchten model the capillary pressure always remains continuous at the interface between the two porous media.

We study now a two-phase flow problem similar to the previous one but with the displacement taking place in the opposite direction that is from the right to the left. The

capillary pressure curves of the Brooks and Corey model show that the capillary pressure always remains continuous and the water saturation in medium 1 stays lower than S^*:

$$TS_{\mathrm{l}} = f(TS_{\mathrm{r}}), \qquad S_{\mathrm{wr1}} \leqslant TS_{\mathrm{l}} \leqslant S^* \tag{53}$$

and

$$p_{\mathrm{c}}(TS_{\mathrm{l}}) = p_{\mathrm{c}}(TS_{\mathrm{r}}) \geqslant p_{\mathrm{d}}^2. \tag{54}$$

These aspects on the capillary pressure–saturation relationship should be introduced in numerical methods. For the mixed hybrid finite elements chosen here to solve the flow equation and the diffusion term in the saturation equation, some slight modifications must be applied. We will present in this paper only the treatment of the saturation discontinuity in the mixed hybrid method.

We consider here only the case where the Brooks and Corey model is used for the p_{c}–S_{w} relationship. For the numerical resolution we take the left-hand side saturation as unknown. This choice is motivated by the fact that once we know the saturation in the coarser porous media having the lower p_{c}–S_{w} curve associated with it, we can determine the saturation in the finer porous media corresponding to the upper curve.

The relationship between TS_{l} and TS_{r} denoting respectively TS_{E,A_i} and TS_{E',A_i} (figure 1) must be introduced on the edges found at the interface between two porous media during the hybridization step of the mixed method. To hybridize the mixed system for a heterogeneous media we use the following properties:

- continuity of the diffusive water flux $Q_{\mathrm{d},E,A_i}^{n+1}$ at time step t^{n+1} through an edge A_i found at the interface of two subdomains of Ω

$$Q_{\mathrm{d},E,A_i}^{n+1} + Q_{\mathrm{d},E',A_i}^{n+1} = 0, \quad \forall A_i,\ A_i \subset \Omega_{\mathrm{l}} \cap \Omega_{\mathrm{m}}; \tag{55}$$

- the relationship between TS_{E,A_i}^{n+1} and TS_{E',A_i}^{n+1} on edge A_i (figure 1) at the interface between two subdomains of Ω:

Case a:

$$TS_{E',A_i}^{n+1} = 1 - S_{\mathrm{nr}} \quad \text{if } TS_{E,A_i}^{n+1} \geqslant S^*, \quad \forall A_i,\ A_i \subset \Omega_{\mathrm{l}} \cap \Omega_{\mathrm{m}} \tag{56}$$

or

$$TS_{E',A_i}^{n+1} = f\big(TS_{E,A_i}^{n+1}\big) \quad \text{if } TS_{E,A_i}^{n+1} < S^*, \quad \forall A_i,\ A_i \subset \Omega_{\mathrm{l}} \cap \Omega_{\mathrm{m}}. \tag{57}$$

Case b:

$$TS_{E',A_i}^{n+1} = f\big(TS_{E,A_i}^{n+1}\big), \quad \forall A_i,\ A_i \subset \Omega_{\mathrm{l}} \cap \Omega_{\mathrm{m}}. \tag{58}$$

We will now derive the expression of function f using the relationship of the Brooks and Corey model. An analysis of the coefficients of function f will be carried out later.

We start by writing the continuity of the capillary pressure:

$$p_{\mathrm{c}}\big(S_{\mathrm{e}2}\big) = p_{\mathrm{c}}\big(S_{\mathrm{e}1}\big) \tag{59}$$

or

$$p_{\mathrm{d}}^{2} S_{\mathrm{e}2}^{-1/\lambda_2} = p_{\mathrm{d}}^{1} S_{\mathrm{e}1}^{-1/\lambda_1}. \tag{60}$$

The effective saturation in medium 2 is given by

$$S_{\mathrm{e}2} = \left(\frac{p_{\mathrm{d}}^{2}}{p_{\mathrm{d}}^{1}}\right)^{\lambda_2} (S_{\mathrm{e}1})^{\lambda_2/\lambda_1}. \tag{61}$$

Using the expression of $S_{\mathrm{e}2}$ (equation (7)), we get

$$\frac{TS_{\mathrm{r}} - S_{\mathrm{wr}2}}{(1 - S_{\mathrm{wr}2} - S_{\mathrm{nr}2})} = \left(\frac{p_{\mathrm{d}}^{2}}{p_{\mathrm{d}}^{1}}\right)^{\lambda_2} (S_{\mathrm{e}1})^{\lambda_2/\lambda_1}, \tag{62}$$

or

$$TS_{\mathrm{r}} = \beta^{\lambda_2} \alpha_2 (S_{\mathrm{e}1})^{\gamma} + S_{\mathrm{wr}2}, \tag{63}$$

with

$$\beta = \left(\frac{p_{\mathrm{d}}^{2}}{p_{\mathrm{d}}^{1}}\right), \qquad \gamma = \frac{\lambda_2}{\lambda_1} \quad \text{and} \quad \alpha_2 = (1 - S_{\mathrm{wr}2} - S_{\mathrm{nr}2}). \tag{64}$$

Replacing the expression of $S_{\mathrm{e}1}$ in (62), the right-hand side saturation TS_{r} can be written with respect to TS_{l} by

$$TS_{\mathrm{r}} = \beta^{\lambda_2} \alpha_2 \left(\frac{TS_{\mathrm{l}} - S_{\mathrm{wr}1}}{\alpha_1}\right)^{\gamma} + S_{\mathrm{wr}2}, \tag{65}$$

or

$$TS_{\mathrm{r}} = \frac{\beta^{\lambda_2} \alpha_2}{\alpha_1^{\gamma}} (TS_{\mathrm{l}} - S_{\mathrm{wr}1})^{\gamma} + S_{\mathrm{wr}2}, \tag{66}$$

or else

$$TS_{\mathrm{r}} = \tau (TS_{\mathrm{l}} - S_{\mathrm{wr}1})^{\gamma} + S_{\mathrm{wr}2}, \tag{67}$$

with

$$\tau = \frac{\beta^{\lambda_2} \alpha_2}{\alpha_1^{\gamma}} \quad \text{and} \quad \alpha_1 = 1 - S_{\mathrm{wr}1} - S_{\mathrm{nr}1}. \tag{68}$$

Function f is nonlinear with coefficients depending on properties of the porous media. In order to study the behavior of f we need to characterize the porous media.

We now refer to the configuration chosen at the beginning. Given the permeabilities chosen for the two porous media, the coefficients in the Brooks and Corey model must respect the following criteria:

$$\begin{cases} \text{permeability of medium 1}, & \lambda_2 < \lambda_1, & (69) \\ > & p_{\mathrm{d}}^{2} > p_{\mathrm{d}}^{1}, & (70) \\ \text{permeability of medium 2}, & S_{\mathrm{wr}2} > S_{\mathrm{wr}1}. & (71) \end{cases}$$

Hence, the coefficients of f respect the following conditions:

$$0 < \gamma = \frac{\lambda_2}{\lambda_1} < 1, \tag{72}$$

$$\beta = \frac{p_{\mathrm{d}}^2}{p_{\mathrm{d}}^1} > 1, \tag{73}$$

$$\alpha_1 < 1 \quad \text{and} \quad \alpha_2 < 1, \tag{74}$$

and

$$\tau = \frac{\alpha_2 \beta^{\lambda_2}}{\alpha_1^{\gamma}} > 0. \tag{75}$$

We just saw that the relationship between the left-hand saturation and the right-hand side one is nonlinear. This nonlinearity of function f is a problem. The matrix system of the mixed hybrid approximation is obtained by writing the continuity of $TS_{E_j}^{n+1}$ for a homogeneous porous media, while we have now a power relationship between TS_{r} and TS_{l}.

The nonlinear system of equations is linearised. We seek the saturation traces at time t^{n+1} and at iteration $k+1$, $TS_{E_j}^{n+1,k+1}$. We already have the saturation traces $TS_{E_j}^{n+1,k}$ of the previous iteration k. The following approximation is then used:

$$\begin{aligned} TS_{\mathrm{r}}^{n+1,k+1} &= \tau\big(TS_{\mathrm{l}}^{n+1,k+1} - S_{\mathrm{wr1}}\big)^{\gamma-1}\big(TS_{\mathrm{l}}^{n+1,k+1} - S_{\mathrm{wr1}}\big) + S_{\mathrm{wr2}} \\ &\approx \tau\big(TS_{\mathrm{l}}^{n+1,k} - S_{\mathrm{wr1}}\big)^{\gamma-1} TS_{\mathrm{l}}^{n+1,k+1} - \tau S_{\mathrm{wr1}}\big(TS_{\mathrm{l}}^{n+1,k} - S_{\mathrm{wr1}}\big)^{\gamma-1} + S_{\mathrm{wr2}}. \end{aligned} \tag{76}$$

3.4. Time and operator splitting applied to the saturation equation

In the saturation equation, we have treated separately advection and diffusion which are modelled by partial differential equations of different nature. An operator splitting can be used to solve advection and diffusion separately [10].

The saturation equation can be written as

$$\begin{aligned} \phi \frac{S_{\mathrm{w}}^{n+1} - S_{\mathrm{w}}^{\mathrm{adv},n+1} + S_{\mathrm{w}}^{\mathrm{adv},n+1} - S_{\mathrm{w}}^{n}}{\Delta t} &= \nabla \cdot (\boldsymbol{h}_{\mathrm{w}} \cdot \nabla S_{\mathrm{w}}) - \nabla \cdot \boldsymbol{G}_{\mathrm{w}} + Q_{\mathrm{w}} \\ &\quad - \nabla \cdot \big(f_{\mathrm{w}}(S_{\mathrm{w}})\boldsymbol{v}_t\big), \end{aligned} \tag{77}$$

where $S_{\mathrm{w}}^{\mathrm{adv},n+1}$ is the water saturation obtained at time step $n+1$ after solving the advection equation with an explicit in time scheme:

$$\phi \frac{S_{\mathrm{w}}^{\mathrm{adv},n+1} - S_{\mathrm{w}}^{n}}{\Delta t} = -\nabla \cdot \big(f_{\mathrm{w}}(S_{\mathrm{w}})\boldsymbol{v}_t\big). \tag{78}$$

Contribution of diffusion, gravity and source/sink terms are taken into account by solving the following equation

$$\phi \frac{S_{\mathrm{w}}^{n+1} - S_{\mathrm{w}}^{\mathrm{adv},n+1}}{\Delta t} = \nabla \cdot (\boldsymbol{h}_{\mathrm{w}} \cdot \nabla S_{\mathrm{w}}) - \nabla \cdot \boldsymbol{G}_{\mathrm{w}} + Q_{\mathrm{w}}. \tag{79}$$

Each diffusive time step is decomposed into n advective time steps:

$$\Delta t = \Delta t_{\text{diff}} = n \Delta t_{\text{adv}}. \tag{80}$$

To solve the saturation equation, we proceed as follows:

- the mean saturation ($\overline{S}_{\text{w}}^{\text{adv},n+1}$) is calculated on each element by solving equation (78) using DFE and a slope limiting procedure. This step is done for the n advective time steps.
- Equation (79) is then discretized using MHFE with an implicit time scheme:

$$\phi |E| \frac{S_{\text{w}}^{n+1} - \overline{S}_{\text{w}}^{\text{adv},n+1}}{\Delta t_{\text{diff}}} = - \int_E \nabla \cdot \boldsymbol{q}_{\text{d},E}^{n+1} - \int_E \nabla \cdot \boldsymbol{G}_{\text{w}}^{n+1} + \int_E Q_{\text{w}}^{n}. \tag{81}$$

Mean saturations on edges are calculated by solving the system of equations of equation (42). The diffusive fluxes and mean saturations on each element is then calculated.

- Saturations on each node are then recalculated by using equation (82). These saturations contain only the effects of advection, we now add diffusive and other effects:

$$S_E^{i,n+1} = S_E^{\text{adv},i,n+1} - \frac{\Delta t_{\text{disp}}}{\phi_E |E|} \left(\sum_{j=1}^{4} Q_{\text{d},E_j}^{n+1} + G_{\text{w},E}^{n+1} \right) = S_E^{\text{adv},i,n+1} + \left(S_E^{n+1} - \overline{S}_E^{\text{adv},n+1} \right) \tag{82}$$

for $i = 1, \ldots, 4$.

4. Model verification

The developed two-phase model is verified through a series of test problems. Four test problems are studied to verify that the model is capable of describing correctly the physics of two-phase and also transport phenomena like advection and diffusion. Rectangular elements are used to discretize the domains for all the test problems treated.

4.1. Test problem No. 1

We first consider the horizontal displacement of oil by water studied by [5]. In this flow problem effects of capillary forces are neglected. Our domain is supposed to be homogeneous. Soil characteristics, fluid properties, Brooks and Corey and simulation parameters are summarised in table 1, test No. 1. The porous media is initially saturated with oil containing water at a residual saturation. In this unidirectional displacement of two incompressible fluids, the total velocity $\boldsymbol{v}_{\text{t}}$ remains constant throughout the domain and is equal to 1.5×10^{-7} m/s.

The saturation profile calculated after 1500 days for several spatial discretisations are represented (figure 3). The saturation profile calculated with a spatial grid of 32 elements is satisfactory with little numerical diffusion. Numerical approximations obtained

Table 1
Parameters used for test problems.

No. 1	
Domain length, cross section	$L = 300$ m, $S = 10$ m^2
BC parameters	$\lambda = 2$, $S_{wr} = 0.2$, $S_{nr} = 0.2$
Fluid properties	$\mu_n = \mu_w = 1.0 \times 10^{-3}$ kg/ms, $\rho_n = \rho_w = 1000$ kg/m^3
Porous media properties	$\phi = 0.2$, $k_{xx} = k_{yy} = 10^{-7}$ m^2
Boundary conditions	S_w ($x = 0$ m)= 0.8, $S_w(x = 300$ m)= 0.2
Initial conditions	$S_w = 0.2$
Spatial discretization	32×9.375 m, 64×4.6875 m, 128×2.34375 m
No. 2	
Domain length, cross section	$L = 2.6$ m, $S = 1$ m^2
BC parameters	$\lambda = 2$, $p_d = 5000$ Nm^{-2}, $S_{wr} = 0$, $S_{nr} = 0$
Fluid properties	$\mu_n = \mu_w = 1.0 \times 10^{-3}$ kg/ms, $\rho_n = \rho_w = 1000$ kg/m^3
Porous media properties	$\phi = 0.3$, $k_{xx} = k_{yy} = 10^{-10}$ m^2
Boundary conditions	$S_w(x = 0$ m$) = 1.0$, $S_w(x = 2.6$ m$) = 0.01$
Initial conditions	$S_w = 0.5$ (in 1st element), $S_w = 0.01$
Spatial discretization	52×0.05 m, 260×0.01 m
No. 3	
Domain length, cross section	$L = 0.3$ m, $S = 1$ m^2
VG parameters	$\alpha = 3.35 \times 10^{-4}$ m^{-1}, $n = 2$, $\theta_r = 0.102$, $\theta_s = 0.368$
Porous media properties	$K_s = 9.22 \times 10^{-5}$ m/s
Boundary conditions	$h(z = 0$ m$) = -10$ m, $h(z = 0.3$ m$) = -0.75$ m
Initial conditions	$h = -10$ m
Spatial discretization	120×0.0025 m
No. 4	
Domain length, cross section	$L = 2$ m, $S = 0.1$ m^2
BC parameters	sand 1: $\lambda = 2$, $p_d = 5000$ Nm^{-2}, $S_{wr} = 0$, $S_{nr} = 0$
	sand 2: $\lambda = 2$, $p_d = 10000$ Nm^{-2}, $S_{wr} = 0$, $S_{nr} = 0$
Fluid properties	$\mu_n = \mu_w = 1.0 \times 10^{-3}$ kg/ms, $\rho_n = \rho_w = 1000$ kg/m^3
Porous media properties	sand 1: $\phi = 0.3$, $k_{xx} = k_{yy} = 10^{-10}$ m^2
	sand 2: $\phi = 0.3$, $k_{xx} = k_{yy} = 2.5 \times 10^{-11}$ m^2
Boundary conditions	$S_w(x = 0$ m$) = 1$, $S_w(x = 2$ m$) = 0$
Initial conditions	$S_w(0$ m $\leqslant x \leqslant 1$ m$) = 1.0$, $S_w(1$ m $< x \leqslant 2$ m$) = 0$
Spatial discretization	80×0.025 m, 400×0.005 m

afterwards for finer grids converge rapidly. The DFE used to solve the advection part of the saturation equation are well suited to treat the nonlinear hyperbolic equation.

4.2. Test problem No. 2

We study the counter-current displacement of oil by water in a horizontal column filled with a homogeneous porous media. Displacement of the oil phase is caused by the capillary pressure gradient at the entrance of the column. The total velocity $\boldsymbol{v}_t$ remains zero during the displacement process, so we need only to solve the diffusive part of the saturation equation. A water saturation of 1.0 is imposed at the entrance of column. The

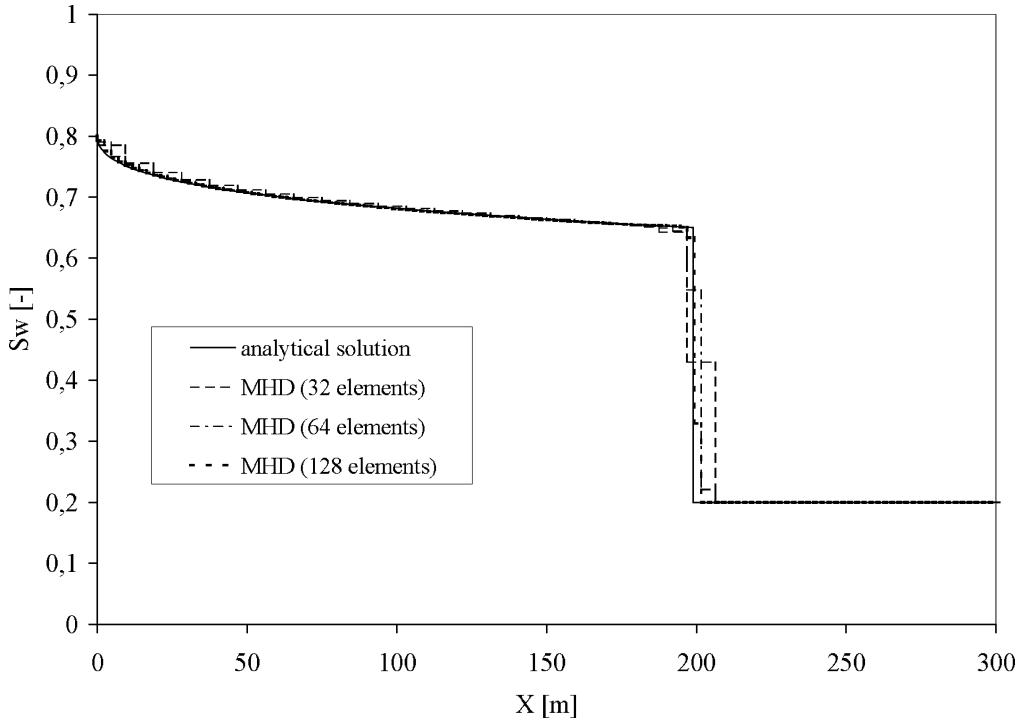

Figure 3. Calculated saturation profiles for different spatial discretisations versus the analytical solution of Buckley and Leverett [5].

other limits of the domain are considered as impermeable. Other simulation parameters and soil characteristics are given in table 1, test No. 2.

Two spatial approximations have been used to evaluate the diffusion associated coefficient (equations (47), (48)). The effects of the approximations made on $\sigma(S_w)$ can be seen on the numerical solution for a coarse grid of 52 elements (figure 4). The saturation profile calculated with approach A (MHDa) are closer to the semi-analytical solution of Mc Whorter and Sunada [15] compared to the one obtained using approach B (MHDb). By using a finer grid, we show that the numerical solution obtained with approach A (MHDa) improves while the one given by approach B remains far away without being able to reproduce the diffusion process (figure 4).

This behaviour of the numerical solution is due the numerical flux which is calculated using a kind of harmonic mean of the diffusion coefficients of the two adjacents elements of the edge on which the flux is evaluated [1]. If we calculate the diffusion associated coefficient ahead of a moving front using the two spatial approximations A and B, we get a greater coefficient σ_E with approach A than by B. This explains why with MHDb, the saturated profile remains sharp and pains to move. If the domain is initially fully saturated with a mean water saturation of 0.5 on the first element, then water enters only in the first element with MHDb while the displacement is correctly calculated with MHDa. We point out here the importance of the initial condition and the

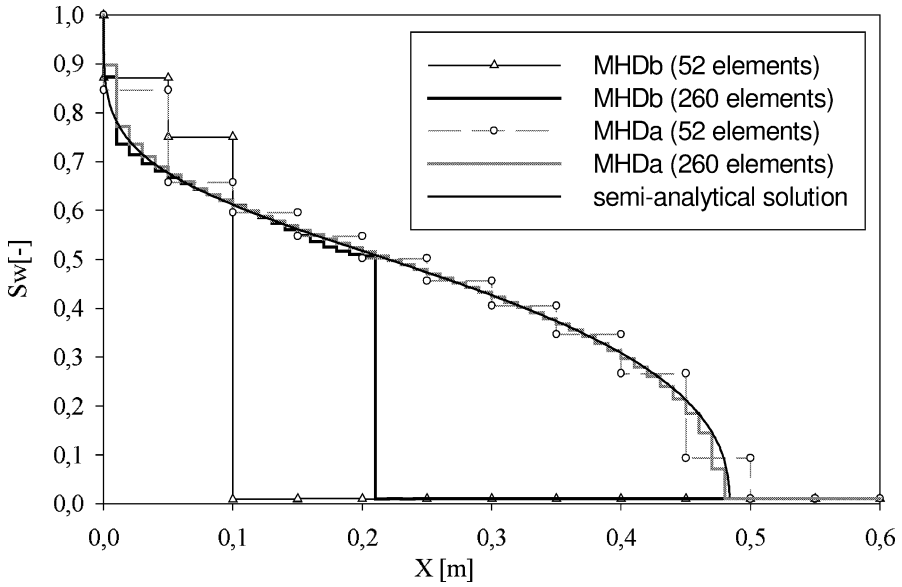

Figure 4. Influence of the diffusion coefficient approximation on the saturation profile calculated for the counter-current problem of Mc Whorter and Sunada [15].

discretization scheme used to approximate the diffusion associated coefficient for this kind of simulation.

4.3. Test problem No. 3

The purpose of this test problem is to simulate the infiltration of water in a vertical column containing sand which is initially dry. The porous medium is considered as homogeneous. This problem whose analytical solution has been given by Philips [18,19] has been studied by several authors [6,13,14,20]. The initial pressure head throughout the column is -1000 cm, and a pressure head of -75 cm and -1000 cm are applied on the top and the bottom of the column respectively. A zero water flux is imposed in the lateral direction. The simulation is carried out for 6 hours. The constitutive relationships of Mualem [16] and Van Genuchten [26] for the unsaturated hydraulic conductivity and the capillary pressure–water content are used respectively (table 1, test No. 3). The space domain is discretized using a grid with $\Delta z = 0.25$ cm. A variable time step is used during the simulations.

Figure 5 shows the calculated water pressure profiles using two spatial approximations to evaluate the hydraulic conductivity, and it is also shown the analytical solution of Philips. The results show that we get a better approximation of the pressure field by using the water pressure values of the element edges to calculate the coefficients in Richards' equation compared to the classical approach.

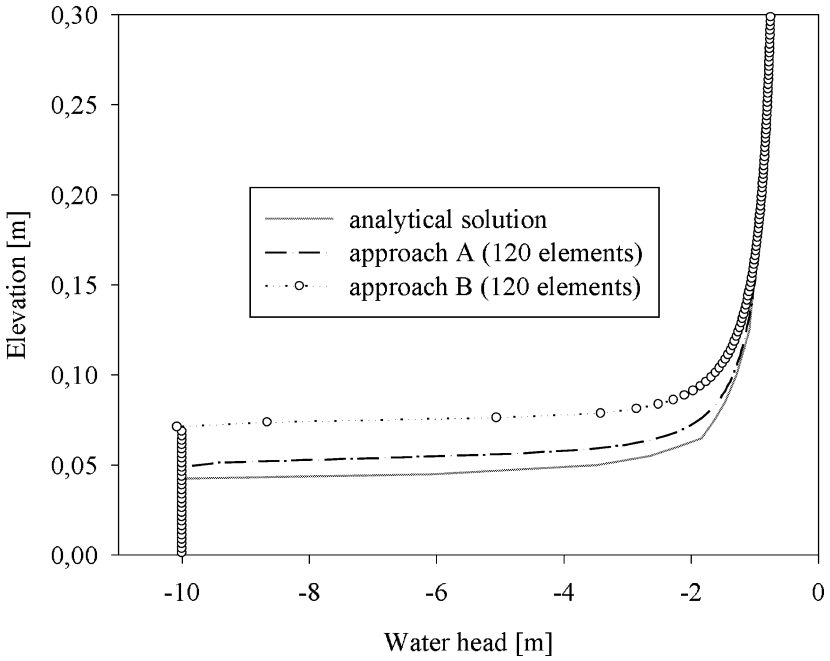

Figure 5. Water pressure head profiles calculated with two spatial approximations of the Richards' equation coefficients versus the analytical solution of Philips [18,19].

4.4. Test problem No. 4

In this test problem we consider a counter-current displacement in heterogeneous porous media. This problem has an analytical solution given by [24,25]. The experimental set up is made up of a horizontal column filled with two sands of different permeability. The left-hand side of the column containing the less permeable sand is initially water saturated and the right-hand side is saturated with oil. The column being closed at its ends, all boundaries are considered as impermeable for the simulation. This displacement problem is also referred to as a redistribution of two immiscible fluids due to capillary forces.

The capillary pressure gradient provokes the displacement of the oil and water phases present on each side of the column. The total velocity remains zero during the whole displacement process. Constitutive relationships of Brooks and Corey are used for the simulation. Coefficients of the BC model, intrinsic permeabilities and porosities of the two sands are given in table 1, test No. 4. We assume that the residual saturations for oil and water are zero.

Fluid properties and parameters used for the simulation are summarized in table 1, test No. 4. The column of length 2 m is divided into two equal parts filled with a coarse and a fine sand. The domain is discretized using two grids, a coarse one (80 elements) and a fine one (400 elements). We assume that oil and water have equal dynamic viscosity.

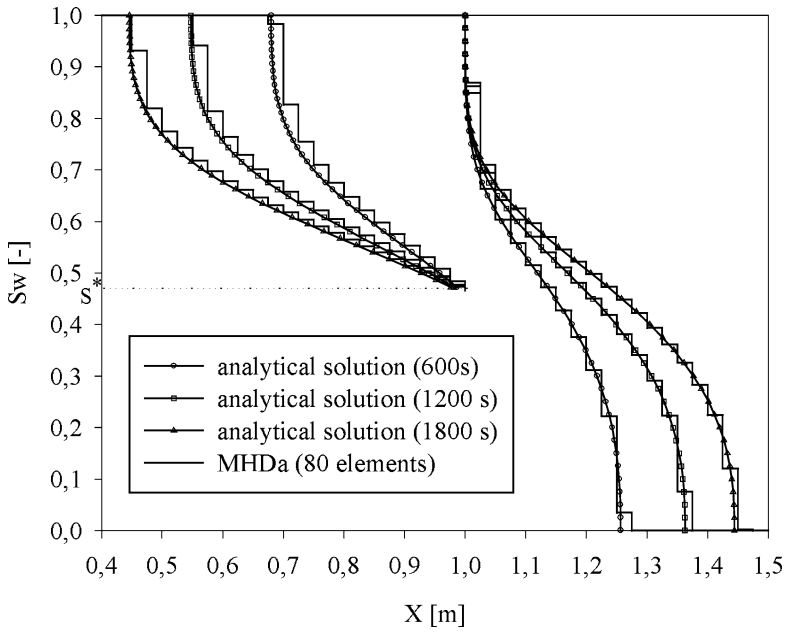

Figure 6. Horizontal counter-current displacement of oil by water in heterogeneous porous media: comparison of the analytical solution of Van Duijn and de Neef [24,25] with the numerical solution obtained with a coarse grid.

The calculated saturation profiles at 600 s, 1200 s and 1800 s for the two discritizations are shown in figures 6 and 7. The calculated saturations match closely with the ones given by the analytical solution. The saturation jump (from S^* to 1) at the limit between the two sands is correctly reproduced. The saturation profile (figure 6) obtained with the coarse grid contains a small numerical diffusion. By refining the grid we verify that the numerical solution (figure 7) improves.

These two simulations have enabled us to verify that the saturation discontinuity at the interface between two porous media is correctly reproduced in the case where the flow is induced only by capillary forces. The numerical solution shows that at the limit between the two sands, the water saturation in the fine sand remains maximum during the whole simulation. This phenomenon is observed as long as the water saturation in the coarse sand remains greater than the critical saturation S^*. We note here that with the Van Genuchten model, we do not have a critical saturation and that the saturations on both sides of the interface depend on each other.

5. Conclusion

In this paper, we have presented a two-phase incompressible flow model capable of simulating the water–air or the water–oil system. For the water–air system, Richards' equation is used to model the two-phase system assuming that the air phase is infinitely

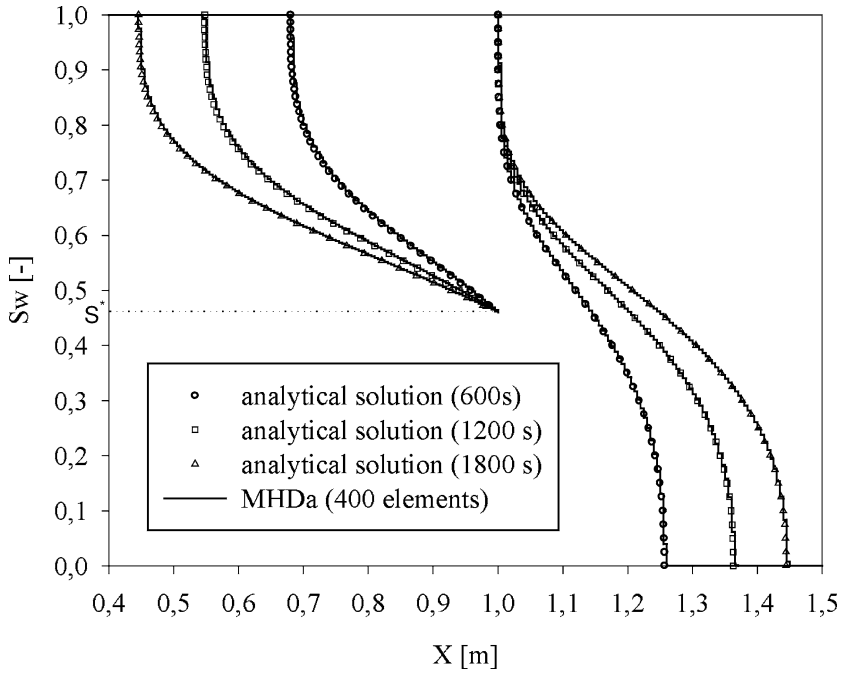

Figure 7. Horizontal counter-current displacement of oil by water in heterogeneous porous media: comparison of the analytical solution of Van Duijn and de Neef [24,25] with the numerical solution obtained with a fine grid.

mobile. The two-phase flow model has been tested for several flow problems involving either advective or diffusive processes. We have shown that the developed two-phase flow simulator is robust and accurate. When using the mixed hybrid finite elements to treat the diffusion term in the saturation equation, the diffusion coefficient need to be evaluated as its average value on the element edges in order to get a physical solution. To handle the discontinuity of the saturation at the interface between two porous media in the MHFE method some modifications have been made. We introduce a relationship which depends on the capillary pressure–saturation function chosen between the saturations on the left and right-hand sides of the interface between the two porous media. Future works will have to verify the two-phase model for flow problems in heterogeneous porous media with advection and taking into account of gravity effects for 1-D and 2-D problems. For the later case, an upwind scheme could be used like in the DFE to define the numerical flux due to gravity uniquely. It should be remarked here that when using the capillary pressure–saturation relationship of Brooks–Corey, the mean pressure may become discontinuous. In this case, a procedure similar to the one used to treat the discontinuity of saturations could be applied in the MHFE method to solve the mean pressure equation. In this work, the developed numerical simulator has been tested only against analytical solutions, comparisons with other two-phase flow models taking into account of CPU time needed will have to be done.

Acknowledgements

Support for this work by a French cooperation scholarship scheme and partly by IFARE (Institut Franco-Allemand de Recherche sur l'Environnement) is gratefully acknowledged by D. Nayagum.

References

[1] Ph. Ackerer, R. Mose and P. Siegel, Reply to the comment on "Application of the mixed hybrid element approximation in a groundwater flow model: Luxury or Necessity?", Water Resour. Res. 32(6) (1996) 1911–1913.
[2] Ph. Ackerer, A. Younes and R. Mosé, Modeling variable flow and solute transport in porous medium: 1. Numerical model and verification, Transport Porous Media 35 (1999) 345–373.
[3] P. Binning and M.A. Celia, Practical implementation of the fractional flow approach to multi-phase flow simulation, Adv. Water Resour. 22(5) (1999) 461–478.
[4] R.H. Brooks and A.T. Corey, Hydraulic properties of porous media, Hydrology Paper 3, Colorado State University, Fort Collins, CO (1964).
[5] S.E. Buckley and M.C. Leverett, Mechanism of fluid displacement in sands, Trans. Amer. Inst. Min. Metall. Petrol. Engrg. 146 (1942) 107–116.
[6] M.A. Celia, E.T. Bouloutas and R.L. Zarba, A general mass-conservative numerical solution for the unsaturated flow equation, Water Resour. Res. 26(7) (1990) 1483–1496.
[7] G. Chavent and J. Jaffré, *Mathematical Models and Finite Elements for Reservoir Simulation*, Studies in Mathematics and its Applications, Vol. 17 (North-Holland, Amsterdam, 1986).
[8] G. Chavent, J. Jaffré and J.E. Roberts, Generalized cell-centered finite volume methods: Application to two-phase flow in porous media, in: *Computational Science for the 21st Century*, eds. M.-O. Bristeau, G. Etgen, W. Fitzgibbon, J.-L. Lions, J. Périaux and M.F. Wheeler (Wiley, Chichester, 1997) pp. 231–241.
[9] P.G. Ciarlet, *Introduction à l'Analyse Numérique Matricielle et à l'Optimisation* (Masson, Paris, 1982).
[10] C.N. Dawson and M.F. Wheeler, Time splitting methods for advection–diffusion-reaction equations arising in contaminant transport, in: *Industrial and Applied Mathematics*, ed. R.E. O'Malley (SIAM, Philadelphia, PA, 1992) pp. 71–80.
[11] L.J. Durlofsky, A triangle based mixed finite element-finite volume technique for modelling two phase flow through porous media, J Comput. Phys. 105 (1993) 252–266.
[12] R.E. Ewing and R.F. Heinemann, Mixed finite elements approximations of phase velocities in compositional reservoir simulation, Comput. Methods Appl. Mech. Engrg. 47 (1984) 161–175.
[13] R. Haverkamp, M. Vauclin, J. Touma, P.J. Wierenga and G. Vachaud, A comparison of numerical simulation models for one-dimensional infiltration, Soil Sci. Amer. J. 41 (1977) 285–294.
[14] F. Lehmann and Ph. Ackerer, Comparison of iterative methods for improved solutions of the fluid flow equation in partially saturated porous media, Transport Porous Media 31(3) (1998) 275–292.
[15] D.B. Mc Whorter and D.K. Sunada, Exact integral solutions for two-phase flow, Water Resour. Res. 26(3) (1990) 399–413.
[16] Y. Mualem, A new model for predicting the hydraulic conductivity of unsaturated porous media, Water Resour. Res. 12 (1976) 513–522.
[17] D. Nayagum, Simulation numérique de la pollution du sous-sol par les produits pétroliers et dérivés: Application au cas d'un écoulement monodimensionnel. Ph.D. thesis, University of Louis Pasteur, Strasbourg, France (2001).
[18] J.R. Philips, The theory of infiltration: 1. The infiltration equation and its solution, Soil Sci. 83 (1957) 345–357.

[19] J.R. Philips, The theory of infiltration: 2. The profile of infinity, Soil Sci. 83 (1957) 435–448.
[20] K. Rathfelder and L. Abriola, Mass conservative numerical solutions of the head-based Richards equation, Water Resour. Res. 30(9) (1994) 2579–2586.
[21] P.A. Raviart and J.M. Thomas, A mixed finite method for the second order elliptic problems, in: *Mathematical Aspects of the Finite Element Methods*, eds. I. Galligani and E. Magenes, Lecture Notes in Mathematics, Vol. 606 (Springer, Berlin, 1977) pp. 292–315.
[22] L.A. Richards, Capillary conduction of liquids through porous mediums, Phys. 1 (1931) 318–333.
[23] P. Siegel, R. Mosé, Ph. Ackerer and J. Jaffré, Solution of the advection dispersion equation using a combination of discontinuous and mixed finite elements, Internat. J. Numer. Methods Fluids 24 (1997) 595–613.
[24] C.J. Van Duijn and M.J. de Neef, Self-similar profiles for capillary diffusion driven flow in heterogeneous porous media, Technical Report AM-R9601, Department of Analysis, Algebra and Geometry, Centrum voor Wiskunde en Informatica, Amsterdam, The Netherlands (1996).
[25] C.J. Van Duijn and M.J. de Neef, Similarity solution for capillary redistribution of two phases in a porous medium with a single discontinuity, Adv. Water Resour. 21 (1998) 451–461.
[26] M.Th. Van Genuchten, A closed-form equation for predicting the hydraulic conductivity of unsaturated soils, Soil Sci. Amer. J. 44 (1980) 892–898.